Terrain Classification using Depth Texture Features

Michael Woods, José Guivant and Jayantha Katupitiya
School of Mechanical and Manufacturing Engineering,
The University of New South Wales, Sydney NSW
{m.woods, j.guivant, j.katupitiya}@unsw.edu.au

Abstract

For Autonomous Ground Vehicles, modelling of the terrain is important for predicting future behaviours and control options. Current terrain modelling is able to identify geometric hazards but has a limited ability to identify complex terrain characteristics. This paper presents a method for segmenting and classifying terrain types based on range data to establish a geometric model of the terrain that maps terrain types to friction coefficients. Segmentation of the depth data is performed by a Piece-Wise Multi-Linear surface approximation, this enables the separation of the dominant surface geometry from the surface material characteristics. Depth texture features that are extracted in this process are used to classify the terrain types, specifically grass, road, dirt, rocks, gravel and sand. Using a Weighted Majority Voting with Dominance classifier, a depth texture only classification accuracy rate of 94.2% was achieved for the different terrain types, with 98.9% for depth and colour descriptors and 92.3% for colour only descriptors.

1 Introduction

Autonomous Ground Vehicles are being used in increasingly more complex and harsh environments because of their ability to replace a human driver and remove them from danger. These situations frequently occur in areas that have unstructured and unknown terrain. Safe and accurate navigation through such environments require predictions of the friction coefficients as well as the dominant surface geometry.

Terrain friction coefficients are known to depend on terrain characteristics such as terrain cohesion and internal friction angle [Iagnemma *et al.*, 2004; Hutangkabodee *et al.*, 2006], whose values are different for different terrain types. Thus, prediction of friction coefficients can be achieved through terrain type classification [Kim *et al.*, 2009; Angelova *et al.*, 2006].

There has been a number of different approaches to terrain classification in recent years, with the three main approaches being, camera only [Brooks and Iagnemma, 2007], LiDAR only and a fusion of both [Häselich *et al.*, 2012] these approaches generally utilise additional sensory data such as accelerometers, GPS and wheel encoders.

Terrain classification using camera only data has been shown to classify terrain well in most environments using colour and image texture data [Jansen *et al.*, 2005; Castano *et al.*, 2001] with reasonable classification rates. However, these methods have to contend with variances in the illumination of the terrain, which in unstructured environments is non-controllable. This may lead to errors in classification when the apparent colours of the terrain do not match up with the expected colours.

LiDAR based terrain classification has been achieved using either range only or a combination of range and remission data, with a majority focusing on the traversability of the terrain which are categorised as road, rough or obstacle terrain type classification. A method that yields good terrain classification accuracies using range and remission data has been developed [Wang *et al.*, 2012], however, the feature descriptors that are used are a high-dimensional set of spatial frequencies of the terrain surface.

The terrain descriptors that have been used include information of the image texture features such as surface roughness [Gadelmawla, 2004] and various spatial frequency features based on the colour image, using texture features generated from the gray-level co-occurrence matrix (GLCM) [Mocofan and Radu, 2013; Woo *et al.*, 2006] and normal colour data.

This paper proposes a novel method for achieving terrain type classification using only range data, allowing for terrain classification to be achieved independent of the ambient lighting conditions and thus be used in conditions where the vision system is not

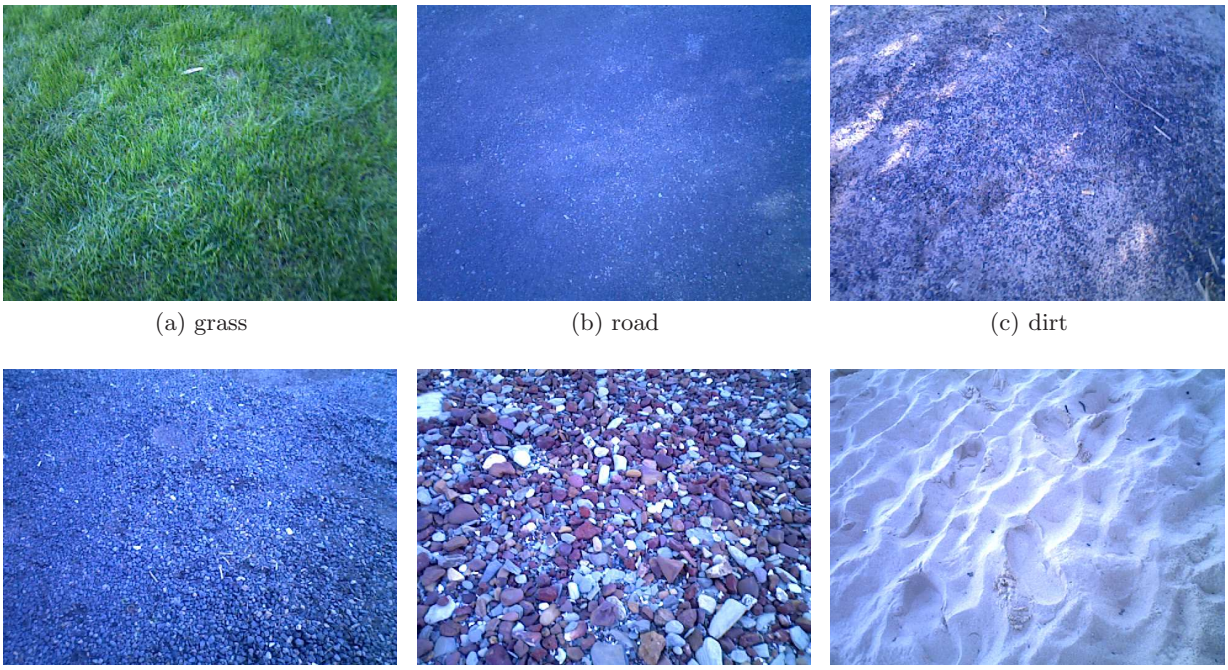

(a) grass (b) road (c) dirt

(d) gravel (e) rock (f) sand

Figure 1: Collect visual data of the terrain types

reliable. The proposed method can also be used to estimate surface boundaries due to the segmentation technique that is developed based on the geometric terrain classification. Additionally, classification combining visual texture information is also shown, and then compared to visual data alone.

2 Approach

In this chapter we introduce the method developed for classifying terrain types using depth data. The depth data is segmented into terrain surfaces, then feature descriptors are generated and an off-line training step is then performed using a previously collected sample set. The classification algorithm then takes in new data to predict the terrain type for new depth data.

A downwards looking PrimeSense Carmine 1.09 was used to collect depth and colour data over a variety of terrain types; grass, road, dirt, gravel, rocks and sand as shown in Fig. 1. The sensor uses structured light to capture depth data from the environment, this method of depth capture is affected heavily by noise from the ambient and direct sunlight so all data was taken in shadowy areas.

The Carmine 1.09 is setup so that it is facing downwards at a shallow angle about 800mm off the ground with a field of view of 57.5x45 at 30Hz sampling rate. The sensor has a depth resolution of 0.1mm and an accuracy of 0.3mm at 600mm distance. The depth data is returned as 640x480 array of depth data as well as colour data.

Segmentation of the depth data allows for the separation of the dominant surface geometry from the surface characteristics or material properties of the surface. This reduces the dimensionality of the depth data so that the physical characteristics and descriptors of a patch of terrain can be easily compared, without the need to include the angle of the terrain.

The segmentation of the data allows for more resolution in terrain classification when identifying boundaries between terrain types. A tree based segmentation method is preferred so that boundaries in 3D space can be easily identified and greater detail can be applied when describing the boundary areas.

2.1 Segmentation

The data segmentation method utilised in this paper is a quad-tree based method and implements a Piece-Wise Multi-Linear (PWML) [Robledo *et al.*, 2011] approximation for surfaces from the 3D data points shown in Fig. 3. The geometric separation of surface planes is shown in Fig. 2. The PWML method allows for the boundaries of these planes to be identified automatically.

The depth data that is gathered by the sensor is registered together with the colour data, so a subset of the depth data is chosen that contains the useable data from the frame.

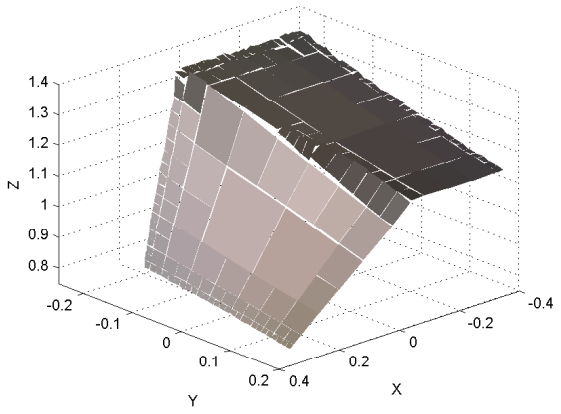

Figure 2: Automatic Piece-Wise Multi-Linear segmentation

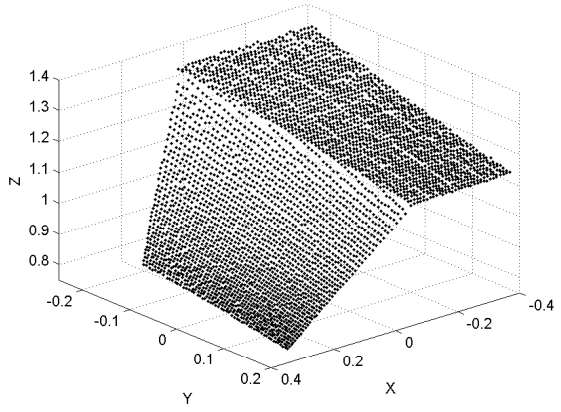

Figure 3: 3D point cloud subsampled by 8 used in PWML segmentation

Once the usable depth data has been identified any missing data in this subset is interpolated using a linear interpolation method. Linear interpolation is adequate for the approach that was taken for collecting data, as most of the depth data is in the shade. This means that there is less interference and so there are no large regions of missing data, which would effect the accuracy of the linear interpolation.

The PWML approximation for 2D surfaces is defined as follows,

$$\begin{gathered} \left|\hat{f}(u,v) - f(u,v)\right| < \tau \\ \forall (u,v) \in \Omega \\ \hat{f}(u,v) = a_k \cdot u \cdot v + b_k \cdot u + c_k \cdot v + d_k \\ \forall (u,v) \in \Omega_k \\ \{\Omega_k\}_{k=1}^{N} \quad / \quad \bigcup_{k=1}^{N} \Omega_k = \Omega \end{gathered} \tag{1}$$

Given a function $f(u,v)$, which is evaluated in the Ω domain, this can be approximated by a Piece-Wise Multi-Linear function $\hat{f}(u,v)$. The Ω domain can be partitioned into square regions $\{\Omega_k\}_{k=1}^{N} \quad / \quad \bigcup_{k=1}^{N} \Omega_k = \Omega$. The $\hat{f}(u,v)$ function is implemented in each region by a multi-linear expression $\hat{f}(u,v) = a_k \cdot u \cdot v + b_k \cdot u + c_k \cdot v + d_k$, with a set of parameters $[a_k, b_k, c_k, d_k]$ describing the surface.

The function $\hat{f}(u,v)$ is calculated for each patch by minimising the error between the patch and the 3D data points. A PWML patch is a valid patch if $\left|\hat{f}(u,v) - f(u,v)\right|$ is less than the threshold value τ else the data set is sub-divided into smaller subsets where the same process repeats until the size of the patch is 8x8 or that a PWML patch can be fitted adequately.

After a PWML patch has been fit to the depth data for a particular region then a matrix containing the discrepancies between the depth data and the PWML patch is generated. The discrepancy between the 3D point cloud and the PWML patch has been visualised from the top and side in Fig. 4 and Fig. 5, the colour of the dots corresponds to how far away a data point is from the plane.

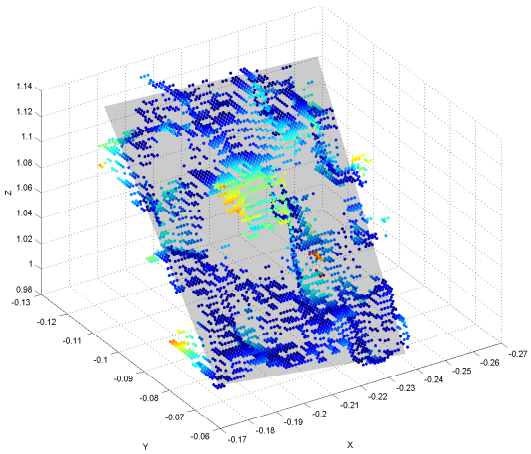

Figure 4: Piece-Wise Multi-Linear patch with residuals top view

These matrices are visualised for one patch for each terrain type in Fig. 6. From the figure it can be seen that there are considerable differences between grass, rock and sand, but there is little difference visually between the road, dirt and gravel terrain types. The discrepancy matrix is then used to generate the depth texture features.

It is assumed that the spatial displacement between adjacent depth data points on the top and bottom rows

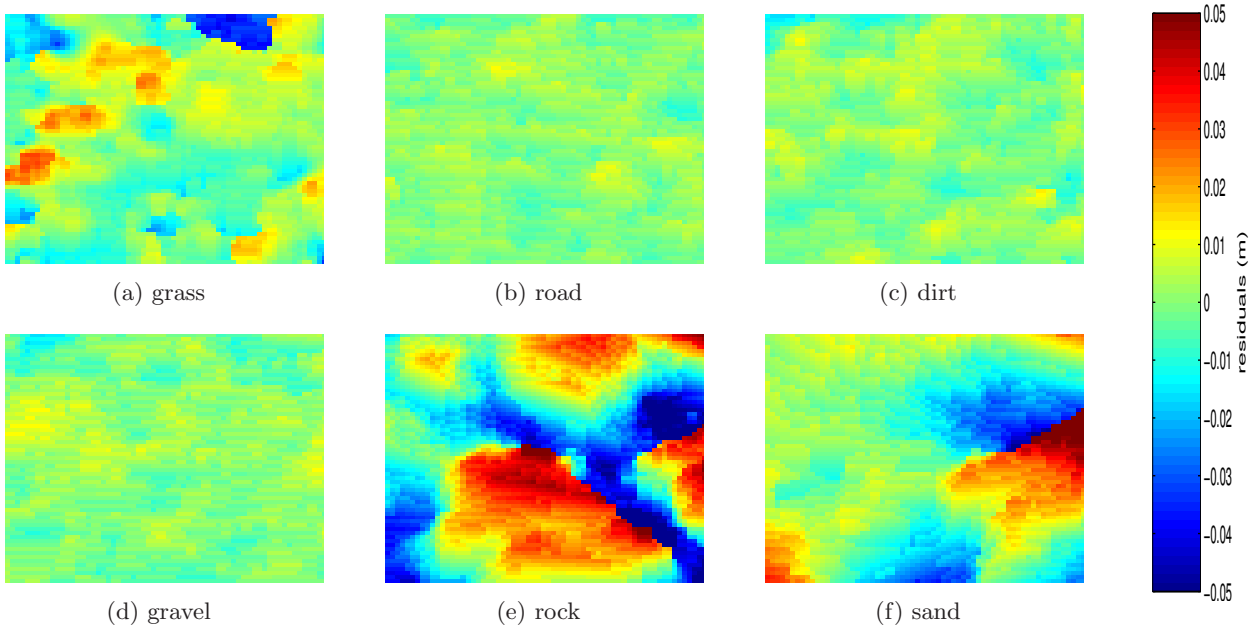

(a) grass (b) road (c) dirt

(d) gravel (e) rock (f) sand

Figure 6: Depth residuals for each terrain type

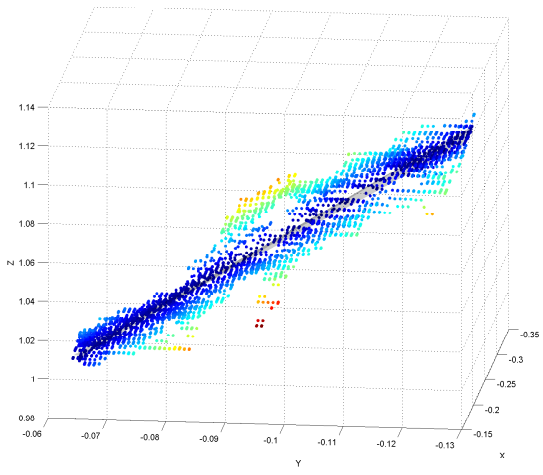

Figure 5: Piece-Wise Multi-Linear patch with residuals side view

of the discrepancy matrix is negligible because the perspective angle of the sensor is small.

2.2 Depth Features

Generally the texture features were developed using a 2D image of a surface [Haralick *et al.*, 1973], with the grayscale image used to look at the texture on the surface. For mobile robotics this approach can work, however this method becomes erroneous when the lighting conditions on the terrain type vary too much from the original dataset that was used for classification.

The main problem with vision based terrain interpretation is that it is heavily relying on either a constant or known lighting condition, and so does not work well under conditions where it is dark or that the image becomes overexposed and so is unusable as well. The colour of the terrain is an easily identifiable feature of a terrain but becomes difficult to include as a feature as the value for a terrain type varies widely due variance in the lighting conditions.

The approach that is used within this paper is to use depth texture data instead of using visual texture data. The depth texture data is generated by using the error matrix that was generated in the previous subsection. A GLCM is then generated from the error matrix.

The depth GLCM is generated by discretising the error matrix into 32 separate levels with 5cm variance about the surface which aligns with the depth resolution of the Carmine sensor. By fixing the number of levels and the separation between levels this allows for easier direct comparison between surfaces that have larger standard deviation on the surface to ones that have a surface that is very flat.

The GLCM provides feature sets from the input data which can be used as a statistical feature for the terrain, the features that were used for the method proposed in this paper are as follows.

1. Standard Deviation

$$f_1 = \sqrt{\frac{1}{N}\sum_{i=1}^{N}(\hat{f}(u,v) - f(u,v))^2} \qquad (2)$$

is the standard deviation of the distances of the 3D points in the chosen region to the PWML patch.

The gray-level co-occurrence matrix as defined in (3) which is used for all subsequent features and is the definition used in [Haralick *et al.*, 1973].

$$p_{\Delta x,\Delta y}(i,j) = \sum_{k=1}^{n}\sum_{l=1}^{n}\begin{cases} 1 & \text{if } I(k,l)=i \text{ and} \\ & I(k+\Delta x, l+\Delta y)=j \\ 0 & \text{otherwise} \end{cases} \quad (3)$$

where Δx and Δy are used to determine the direction that the specific gray-level co-occurrence matrix is based on.

2. Contrast
$$f_2 = \sum_{i,j} |i-j|^2 p(i,j) \quad (4)$$

3. Correlation
$$f_3 = \sum_{i,j} \frac{(i-\mu_x i)(j-\mu_y j)p(i,j)}{\sigma_x \sigma_y} \quad (5)$$

4. Homogeneity
$$f_4 = \sum_{i,j} \frac{p(i,j)}{1+|i-j|} \quad (6)$$

5. Information Measure of Correlation
$$f_5 = \frac{HXY - HXY1}{max\{HX, HY\}} \quad (7)$$
where HX and HY are entropies of p_x and p_y respectively as shown in [Haralick *et al.*, 1973] and
$$HXY = -\sum_{i,j} p(i,j) log(p(i,j)) \quad (8)$$
$$HXY1 = -\sum_{i,j} p(i,j) log(p_x(i)p_y(j)) \quad (9)$$

6. Maximum Probability
$$f_6 = max\{p(i,j)\} \quad (10)$$
The maximum probability feature is a measure of the most common gray-level co-occurrence throughout the region.

7. Dissimilarity
$$f_7 = \sum_{i,j} p(i,j)|i-j| \quad (11)$$

These features have been chosen so as to maximise the classification rate of the classifiers, the list of features shown above have the greatest level of distinction between terrain type groups. The texture features that are used in the classification are the maximum value for the feature type for all four distinct combinations of Δx and Δy with a distance of 1 grid.

2.3 Visual Features

The lighting conditions of the environment affects the perceived colour of the terrain, however, there are still some features that can be extracted from the data that are partially independent of the ambient conditions. These optional features can be used to improve the terrain classification results under reasonable lighting conditions. The features that have been used in this paper are the GLCM texture properties as shown in (4), (5), (6) and (11) with the data source being a grayscale conversion of the colour information of the region.

3 Terrain Classification

This paper employs a multi-variate classification fusion system that fuses the outputs of three different classifier methods together. The output of the fusion algorithm has been shown to generate results that are better than any one of the classifiers combined [Tamilselvan *et al.*, 2013].

3.1 Weighted Majority Voting with Dominance

The algorithm is called Weighted Majority Voting with Dominance (WMVD) and the implementation relies on the evaluation of classification accuracy. The validation method used is a k-Fold cross validation, with the original data set being split into k mutually exclusive subsets. One of the subsets is used for validation and the other k-1 are used for training.

$$CC_{ij} = \begin{pmatrix} d_{1,1} & \cdots & d_{1,c} \\ \vdots & \ddots & \vdots \\ d_{r,1} & \cdots & d_{r,c} \end{pmatrix} \quad (12)$$

$$AC_{ij} = \begin{pmatrix} a_1, \vdots, a_r \end{pmatrix}^T \quad (13)$$

The index i represents the subset, the index j represents the descriptor number, the index m represents the classifier function and index l represents the data points in a subset and ranges from 1 to r. The matrix CC_{ij} represents the classifier decision of the jth terrain type for the ith subset, where $d_{l,m}$ is the classifier decision of the mth classifier for the lth training point. The vector AC_{ij} represents the target classification for

the jth terrain type with for the ith subset and a_l is the target classification for the lth training point.

The accuracy of prediction for the individual classification functions are then measured against the true results. (14) shows that if the classifier results are true then its corresponding R term is 1, otherwise the term is 0.

$$R(CC_{ij}(l,m), AC_{ij}(l,1)) = \begin{cases} 1 & \text{if } CC_{ij}(l,m) = AC_{ij}(l,1) \\ 0 & \text{otherwise} \end{cases} \quad (14)$$

The R value is then used to determine the classification index χ_{mj}, for each classifier and each descriptor. The values of χ_{mj} are then used to determine the weight of the contribution of each member algorithm in the WMVD approach. The value of χ_{mj} is calculated as shown in (15).

$$\chi_{mj} = \frac{1}{kr} \sum_{i=1}^{k} \left[\sum_{l=1}^{r} R(CC_{ij}(l,m), AC_{ij}(l,1)) \right] \quad (15)$$

from the value of χ_{mj} the weight of the mth member algorithm is determined. The normalised weight wt_{mj} is determined based on (16), which is dependant on the current training data set. If wt_{mj} needs to be updated then additional members need to be added to the training data set to be able to generate a new normalised weight.

$$wt_{mj} = \frac{\chi_{mj}}{\sum_{j=1}^{n} \sum_{m=1}^{c} \chi_{mj}} \quad (16)$$

The classification output of the WMVD for the next data point is then calculated based on the individual predictions for each of the classifiers used. This is then collated into the form of inc_{mj} as shown in (17)

$$inc_{mj} = \begin{cases} 1 & \text{if classifier m classified the incoming} \\ & \text{point as the } j\text{th terrain type} \\ 0 & \text{otherwise} \end{cases} \quad (17)$$

The incoming prediction results inc_{mj} are then combined with the normalised weighting wt_{mj} of the individual classifiers as shown in (18).

$$T_j = \sum_{m=1}^{c} wt_{mj} inc_{mj} \quad (18)$$

The class j that corresponds to the maximum value of the weighted sum T_j is determined to be the class of the terrain surface that is being evaluated.

The three classifiers that are combined together in the WMVD classifier are the k-Nearest Neighbour classifier with k = 5, a probability based Mahalanobis distance classifier and a decision tree classifier.

k-Nearest Neighbours
The k-Nearest Neighbours classifier operates by being given a known sample set and then comparing any new samples to this set and performing a weighted average of the k nearest neighbours to the new sample to estimate the terrain type, which in our implementation utilises a Mahalanobis distance metric for determining the nearest neighbours to the new point.

Mahalanobis
The Mahalanobis distance (19) is a unitless measure of how close a sample is to a known sample set. The distance measure accounts for correlations in the data set and can be used in a multivariate feature space where the features have correlation and whose units are not equal in their distribution.

$$D_M = \sqrt{(X - \mu_k)\Sigma_k^{-1}(X - \mu_k)} \quad (19)$$

where μ_k and Σ_k are the mean and covariance of the kth group

Decision Tree
The decision tree classifier generates a number of discrete rules for classification using the test data, from there classification is done by comparing the features in the descriptor to that in the branches of the tree and this is done until a leaf of the decision tree has been found.

4 Results

The results of the depth feature only terrain classification can be seen in Table 1. These results are for the WMVD classification method and show that there is correlation between the terrain types namely; road, dirt and gravel as well as rocks and sand.

The misclassification of sand and rocks can be attributed to the sand dunes that can be seen in Fig. 1f, showing that the dominant surface geometry of the sand dune was still present in the data. The surfaces, road, dirt and gravel are very similar as shown in Fig. 6.

The correlation between the terrain types; road, dirt and gravel as well as rock and sand, can be seen in the depth feature values, where there is significant overlap in the values of the descriptors. This is mainly due to physical similarities in the terrains themselves.

The individual classification results can be seen in Table 2. The classifiers are successfully able to identify the grass terrain type, with the results for the other terrain types still giving good classification. The

	Grass	Road	Dirt	Rock	Gravel	Sand
Grass	99.9	0	0	0	0	0
Road	0	87.6	8.2	0	4.1	0
Dirt	0	4.2	94.8	0	1.0	0
Rock	0	0	0	95.8	0	4.2
Gravel	0	2.0	2.0	0	96.1	0
Sand	0	0	0	9.3	0	90.7
Average Accuracy: 94.2%						

Table 1: Depth only WMVD Classification results

WMVD classifier shows that it is able to combine the individual classifiers together effectively so that a better overall terrain type classification can be achieved.

	kNN	Maha	DT	WMVD
Grass	99.9	98.7	99.9	99.9
Road	89.9	76.9	82.3	87.6
Dirt	93.4	73.7	85.3	94.8
Gravel	92.1	86.8	78.5	95.8
Rock	90.7	73.7	87.3	96.1
Sand	92.3	62.5	90.1	90.7
Total	93.1	78.7	87.2	94.2

Table 2: True positive classification results

	Grass	Road	Dirt	Rock	Gravel	Sand
Grass	99.9	0	0	0	0	0
Road	0	98.0	0	0	2.0	0
Dirt	0	0	99.0	0	1.0	0
Rock	0	0	0	99.0	1.0	0
Gravel	0	1.9	0	0	98.1	0
Sand	0	0	0	0	0	99.9
Average Accuracy: 98.9%						

Table 3: Depth and colour data WMVD Classification results

With the inclusion of four additional features the classification rate can be improved to 98.9% accuracy shown in Table 3, these features are the Contrast, Correlation, Homogeneity and Dissimilarity of the visual data as outlined in section 2.3. These features are only partially susceptible to the ambient lighting conditions and so can be used when the lighting conditions are not in their extremes. The results of using both the depth and the visual feature descriptors together can be seen in Table 4

Utilising only the four visual texture features from section 2.3 the total accuracy for the classification is 92.3% shown in Table 4, using the same method of classification as with the depth only and the depth and visual data classification. This results reveals that using depth only features can be as effective or better at

	kNN	Maha	DT	WMVD
Grass	99.9	99.9	99.0	99.9
Road	95.7	94.1	97.5	97.7
Dirt	99.9	87.5	91.9	96.0
Gravel	99.9	97.9	82.4	99.9
Rock	95.8	94.4	95.2	99.9
Sand	99.9	99.9	97.9	99.9
Total	98.6	95.6	94.0	99.0

Table 4: True positive classification results including visual texture descriptors

terrain type classification than visual texture features.

	Grass	Road	Dirt	Rock	Gravel	Sand
Grass	93.0	0	3.5	0	3.5	0
Road	2.8	90.3	4.1	0	2.8	0
Dirt	2.8	0	93.4	0	3.8	0
Rock	0	0	2.8	90.6	6.6	0
Gravel	5.0	6.1	0	0	88.9	0
Sand	0	2.2	0	0	0	97.8
Average Accuracy: 92.3%						

Table 5: Colour only WMVD Classification results

5 Conclusion

This paper has presented a method for segmenting and classifying terrain types based on range data. The segmentation was carried out using a Piece-Wise Multi-Linear approximation to a subset of 3D point cloud data points which allows for the separation of the dominant surface geometry from the surface material characteristics. The PWML patches that are found from this method are used to create discrepancy matrices, which are used in a new application of textural features are employed to generate texture features using the range data.

Three separate classifiers are then implemented to classify the six terrain types with a Weighted Majority Voting with Dominance combinational classifier combining the classification results of the three individual classifiers to yield better classification results.

With the use of only depth texture features an overall terrain classification accuracy of 94.2% is achieved on the six different terrain types. With each terrain type a friction coefficient can be assigned to each patch via a lookup table, allowing for improved controllability over a surface. The terrain classification accuracy can be further improved by including four additional colour texture features which results in a classification accuracy of 98.9%, and colour only classification has an accuracy of 92.3%.

6 Future Work

The final goal of this research is to enable an AGV to operate in an unknown environment with the classifier able to identify when a new terrain type has been encountered and then incorporate the new terrain into its database. A different segmentation method is to be implemented based not only on geometry of the PWML patch but also on the depth texture features sampled at each depth data point, this will reduce the correlation issue with the terrain depth feature values overlapping as additional information will be available including the neighbourhood depth feature values.

An online implementation of the segmentation and classification method would then be implemented and installed onto one of the AGVs at UNSW so that the perception algorithm can be tested under real world environments. An implementation of this method is also planned, which will use a 3D laser scanner system in place of the RGBD camera so that this method can be implemented in outdoors settings.

References

[Angelova *et al.*, 2006] Anelia Angelova, Larry Matthies, Daniel Helmick, and Pietro Perona. Slip prediction using visual information. *In Proceedings of Robotics Science and Systems*, 12:15, 2006.

[Brooks and Iagnemma, 2007] C.A. Brooks and K.D. Iagnemma. Self-supervised classification for planetary rover terrain sensing. In *Aerospace Conference, 2007 IEEE*, pages 1–9, 2007.

[Castano *et al.*, 2001] Rebecca Castano, Roberto Manduchi, and Justin Fox. Classification experiments on real-world texture. In *Third Workshop on Empirical Evaluation Methods in Computer Vision, Kauai, Hawaii, December 10, 2001.* Pasadena, CA: Jet Propulsion Laboratory, National Aeronautics and Space Administration, 2001., 2001.

[Gadelmawla, 2004] E.S. Gadelmawla. A vision system for surface roughness characterization using the gray level co-occurrence matrix. {*NDT*} *& E International*, 37(7):577 – 588, 2004.

[Haralick *et al.*, 1973] R.M. Haralick, K. Shanmugam, and Its'Hak Dinstein. Textural features for image classification. *Systems, Man and Cybernetics, IEEE Transactions on*, SMC-3(6):610–621, 1973.

[Häselich *et al.*, 2012] Marcel Häselich, Marc Arends, Nicolai Wojke, Frank Neuhaus, and Dietrich Paulus. Probabilistic terrain classification in unstructured environments. *Robotics and Autonomous Systems*, 2012.

[Hutangkabodee *et al.*, 2006] Suksun Hutangkabodee, YahyaHashem Zweiri, LakmalDasarath Seneviratne, and Kaspar Althoefer. Soil parameter identification for wheel-terrain interaction dynamics and traversability prediction. *International Journal of Automation and Computing*, 3(3):244–251, 2006.

[Iagnemma *et al.*, 2004] K. Iagnemma, Shinwoo Kang, H. Shibly, and S. Dubowsky. Online terrain parameter estimation for wheeled mobile robots with application to planetary rovers. *Robotics, IEEE Transactions on*, 20(5):921–927, 2004.

[Jansen *et al.*, 2005] P. Jansen, W. van der Mark, J.C. van den Heuvel, and F.C.A. Groen. Colour based off-road environment and terrain type classification. In *Intelligent Transportation Systems, 2005. Proceedings. 2005 IEEE*, pages 216–221, 2005.

[Kim *et al.*, 2009] Jayoung Kim, D. Kim, Jonghwa Lee, Jihong Lee, H. Joo, and In-So Kweon. Non-contact terrain classification for autonomous mobile robot. In *Robotics and Biomimetics (ROBIO), 2009 IEEE International Conference on*, pages 824–829, 2009.

[Mocofan and Radu, 2013] Muguras Mocofan and Vasiu Radu. A 3d approach to co-occurrence matrix features used in dynamic textures indexing. In *Advanced Engineering Forum*, volume 8, pages 516–526. Trans Tech Publ, 2013.

[Robledo *et al.*, 2011] Alicia Robledo, Stephen Cossell, and Jose Guivant. Outdoor ride: Data fusion of a 3d kinect camera installed in a bicycle. In *Proceedings of the 2011 Australasian Conference on Robotics & Automation, Melbourne, Australia*, 2011.

[Tamilselvan *et al.*, 2013] Prasanna Tamilselvan, Pingfeng Wang, and Michael Pecht. A multi-attribute classification fusion system for insulated gate bipolar transistor diagnostics. *Microelectronics Reliability*, 53(8):1117 – 1129, 2013.

[Wang *et al.*, 2012] Shifeng Wang, Sarath Kodagoda, and Ravindra Ranasinghe. Road terrain type classification based on laser measurement system data. *Proceedings of the 2012 Australasian Conference on Robotics & Automation*, 2012.

[Woo *et al.*, 2006] Dong-Min Woo, Dong-Chul Park, Seung-Soo Han, and Quoc-Dat Nguyen. Application of 3d co-occurrence features to terrain classification. In Long-Wen Chang and Wen-Nung Lie, editors, *Advances in Image and Video Technology*, volume 4319 of *Lecture Notes in Computer Science*, pages 305–313. Springer Berlin Heidelberg, 2006.